AMERICAN SOCIETY FOR MICROBIOLOGY | Applied and Environmental Microbiology

Mycology | Full-Length Text

The white rot basidiomycete *Gelatoporia subvermispora* produces fatty aldehydes that enable fungal manganese peroxidases to degrade recalcitrant lignin structures

Alexander N. Kapich,[1] Hideki Suzuki,[1] Kolby C. Hirth,[1] Elena Fernández-Fueyo,[2] Angel T. Martínez,[2] Carl J. Houtman,[1] Kenneth E. Hammel[3]

AUTHOR AFFILIATIONS See affiliation list on p. 14.

ABSTRACT The ability of some white rot basidiomycetes to remove lignin selectively from wood indicates that low molecular weight oxidants have a role in ligninolysis. These oxidants are likely free radicals generated by fungal peroxidases from compounds in the biodegrading wood. Past work supports a role for manganese peroxidases (MnPs) in the production of ligninolytic oxidants from fungal membrane lipids. However, the fatty acid alkylperoxyl radicals initially formed during this process are not reactive enough to attack the major structures in lignin. Here, we evaluate the hypothesis that the peroxidation of fatty aldehydes might provide a source of more reactive acylperoxyl radicals. We found that *Gelatoporia subvermispora* produced *trans*-2-nonenal, *trans*-2-octenal, and n-hexanal (a likely metabolite of *trans*-2,4-decadienal) during the incipient decay of aspen wood. Fungal fatty aldehydes supported the *in vitro* oxidation by MnPs of a nonphenolic lignin model dimer, and also of the monomeric model veratryl alcohol. Experiments with the latter compound showed that the reactions were partially inhibited by oxalate, the chelator that white rot fungi employ to detach Mn^{3+} from the MnP active site, but nevertheless proceeded at its physiological concentration of 1 mM. The addition of catalase was inhibitory, which suggests that the standard MnP catalytic cycle is involved in the oxidation of aldehydes. MnP oxidized *trans*-2-nonenal quantitatively to *trans*-2-nonenoic acid with the consumption of one O_2 equivalent. The data suggest that when Mn^{3+} remains associated with MnP, it can oxidize aldehydes to their acyl radicals, and the latter subsequently add O_2 to become ligninolytic acylperoxyl radicals.

IMPORTANCE The biodegradation of lignin by white rot fungi is essential for the natural recycling of plant biomass and has useful applications in lignocellulose bioprocessing. Although fungal peroxidases have a key role in ligninolysis, past work indicates that biodegradation is initiated by smaller, as yet unidentified oxidants that can infiltrate the substrate. Here, we present evidence that the peroxidase-catalyzed oxidation of naturally occurring fungal aldehydes may provide a source of ligninolytic free radical oxidants.

KEYWORDS white rot fungus, free radicals, ligninolysis, fatty aldehydes, manganese peroxidase

Lignin, an aromatic polyether that protects the structural cellulose and hemicelluloses of vascular plants from attack by most microbes, is degraded via oxidative mechanisms by basidiomycete fungi that cause white rot of wood. Fungal ligninolysis is important both for global carbon cycling and for potential biotechnological applications aimed at recovering the valuable cellulose. In the latter case, the ability of some white rot fungi to degrade much of the lignin within the wood cell wall before they attack the

Editor Yvonne Nygård, Chalmers tekniska hogskola AB, Gothenburg, Sweden

Address correspondence to Kenneth E. Hammel, kehammel@wisc.edu.

The authors declare no conflict of interest.

See the funding table on p. 14.

Received 15 November 2023
Accepted 26 February 2024
Published 14 March 2024

cellulose is of particular interest. This process, in which ligninolysis and cellulose removal are temporally separated, is called selective delignification (1, 2).

The arsenal of ligninolytic agents that white rot fungi use has not been fully identified, although it is evident that relatively strong oxidants are required because most lignin subunits lack strongly electron-donating phenolic substituents (3). Specialized peroxidases are essential components of the ligninolytic system, and some of them likely attack lignin via direct contact at the wood cell wall surface (4, 5). However, selective delignification must occur at a distance from these enzymes because the porosity of the intact wood cell wall is too low for them to infiltrate (2). Accordingly, low molecular weight oxidants are presumably responsible for initiating selective white rot. These agents must be relatively nonselective, given the stereoirregular structure of lignin (3), and consequently are likely to be free radicals.

Most research on routes for the production of these hypothetical small oxidants has focused on the peroxidases, which consist of lignin peroxidases, manganese peroxidases (MnPs), and some enzymes (called versatile peroxidases) that combine properties of both (4, 5). Lignin peroxidases can oxidize nonphenolic lignin structures directly, but appear unable to produce diffusible oxidants that could act remotely (6). MnPs and versatile peroxidases oxidize Mn^{2+} to Mn^{3+}, which is chelated under physiological conditions with oxalate, a fungal metabolite that facilitates MnP turnover by chelating Mn^{3+} to promote its release from the enzyme (7, 8). Manganic oxalate chelates are mild, diffusible oxidants that can attack the minor phenolic structures in lignin (9), but there is no evidence that they can oxidize the polymer's predominant nonphenolic structures.

However, MnP exhibits a higher reactivity in the presence of peroxidizable fatty acids. These reactions result not only in oxidative degradation of the lipids, but also in the co-oxidation of various recalcitrant substrates. The latter include lignin and lignin model compounds, polyaromatic hydrocarbons, and other xenobiotics (10–15). A variety of unsaturated lipids have been shown to promote these reactions, including linoleic acid, the principal fatty acid in white rot fungal cell membranes (16), as well as more specialized fungal lipids such as ceriporic acids (17). Whether these co-oxidations occur *in vivo* has not been elucidated, but the high extent of lipid peroxidation found in mycelia of white rot fungi indicates that they are likely (16). Possibly also relevant is the observation that genes encoding the biosynthesis of unsaturated fatty acids are upregulated when some white rot fungi are cultured on wood (18).

Since lipid peroxidation results in the formation of peroxyl radicals, which are moderately strong, diffusible oxidants, it might provide a route for fungal ligninolysis. However, a difficulty with this hypothesis is that the initial steps in fatty acid peroxidation, namely abstraction of a methylene hydrogen followed by isomerization to give a conjugated diene and subsequent addition of O_2 (Fig. 1), can be replicated simply by adding chelated Mn^{3+} to linoleic acid, yet this process fails to cleave nonphenolic lignin model compounds (19). Accordingly, the alkylperoxyl radicals initially produced during the peroxidation of the most abundant fungal fatty acid are not reactive enough to degrade lignin.

A possible clue to the problem comes from two prior observations. First, some synthetic peroxyl radicals bearing electron-withdrawing substituents appear to be directly ligninolytic (20). Second, substrate co-oxidation does not occur immediately when MnP and Mn^{2+} are combined with unsaturated fatty acids. Instead, it begins after a lag of several hours, coinciding with the production of late-stage lipid peroxidation products (19). Prominent among these products are fatty aldehydes that result from the oxidative scission of fatty acids (21). Fatty aldehydes are also produced by some basidiomycetes as secondary metabolites rather than as products of fatty acid peroxidation (22–24).

Fatty aldehydes are potential sources of peroxyl radicals that carry activating groups, because the most facile route for one-electron oxidation of an aldehyde is abstraction of the carbonyl hydrogen to give an acyl radical (25). Rapid (diffusion-limited) addition of O_2 to this radical then yields an acylperoxyl radical (Fig. 1), whose electron-withdrawing

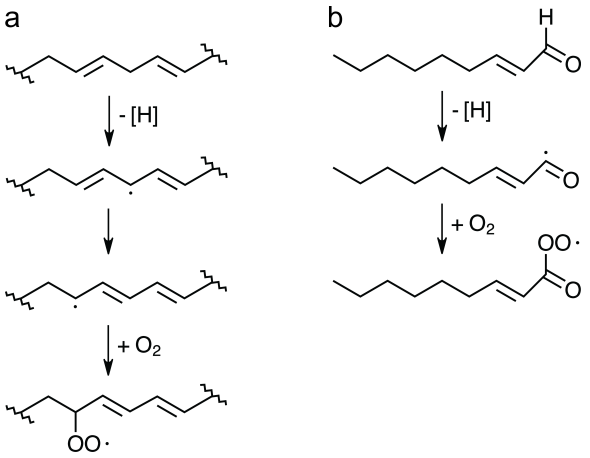

FIG 1 Pathways for formation of peroxyl radicals via hydrogen abstraction. (a) Formation of an alkylperoxyl radical from linoleic acid, showing only the diene portion of the molecule. (b) Formation of an acylperoxyl radical from an aldehyde, showing *trans*-2-nonenal.

carbonyl group makes it more oxidizing than an alkylperoxyl radical (26, 27). If fatty aldehydes were to occur on wood undergoing selective white rot, and if MnPs were to catalyze their one-electron oxidation, an ongoing supply of ligninolytic acylperoxyl radicals might result. In support of this sequence, acyl radicals were previously reported to occur when MnP oxidizes linoleic acid *in vitro* (28).

Gelatoporia (formerly *Ceriporiopsis*) *subvermispora* is probably the most intensively studied selective white rot fungus. Here, we present evidence (i) that *G. subvermispora* produces fatty aldehydes and MnP activity when growing on wood, (ii) that MnPs co-oxidize nonphenolic lignin structures in the presence of fatty aldehydes, (iii) that MnPs oxidize one of the major *G. subvermispora* aldehydes to a carboxylic acid, the expected end product if an acylperoxyl radical is initially produced, and (iv) that the stoichiometry of this oxidation is consistent with the intermediacy of acylperoxyl radicals. Finally, we outline a hypothesis that attempts to reconcile these findings with previous research literature on the MnP catalytic cycle.

RESULTS

MnP activity and fatty aldehydes in colonized wood

We grew *G. subvermispora* on aspen chips in the presence of an auxiliary carbon source. This approach, used previously for the biological pulping of wood, elicits ligninolysis by *G. subvermispora* (29, 30). During the first few weeks of white rot by this fungus, wood polysaccharides remain mostly intact and little weight loss occurs (1, 2). After 4 weeks of colonization, the dry weight loss in our cultures was 4.3 ± 1.6%, and at 8 weeks, it was 5.2 ± 1.3% (sample SD, $n = 6$). Since extractives had been removed from the wood before inoculation with *G. subvermispora*, the weight losses can be attributed to an incipient loss of wood polymers. Our results align with those reported previously for this fungus grown on wood under biopulping conditions (31).

MnP activity was present in the colonized wood at weeks 4 and 8 (Table 1). With regard to fatty aldehydes that might occur in the wood following the peroxidation of fungal membrane lipids, two likely candidates were *trans*-2,4-decadienal and n-hexanal. *trans*-2,4-Decadienal is the major aldehyde initially formed during the peroxidative cleavage of linoleic acid. *trans*-2,4-Decadienal is then further peroxidized in subsequent reactions that yield n-hexanal, which is often used as a marker of linoleic acid peroxidation (21). In addition, we looked for three fatty aldehydes that have been found in the fruiting bodies of other basidiomycetes: *trans*-2-octenal, *trans*-2-nonenal, and *trans*-2-decenal (22–24).

TABLE 1 Fatty aldehydes, ergosterol, and MnP activity found in aspen wood colonized by *G. subvermispora*

Conditions	MnP activity (U g^{-1} wood)[a]	Lipid concentrations in replicate cultures (pmol g^{-1} wood)[b]			
		Ergosterol	Fatty aldehydes		
			trans-2-Nonenal	*trans*-2-Octenal	n-Hexanal
Non-inoculated	ND[c]	ND	ND	ND	640
					310
					282
Inoculated, 4 weeks	1.74 ± 0.12	3,063	166	61	922
		3,271	249	96	1,315
		3,761	200	66	949
Inoculated, 8 weeks	1.69 ± 0.07	5,878	138	98	953
		4,394	78	68	736

[a]Averages ± SD of the sample for triplicate cultures. Each culture (originally containing 10 g oven-dry wood) was extracted with aqueous buffer as described in Materials and Methods.
[b]Data for individual cultures are shown. Each culture (originally containing 10 g oven-dry wood) was extracted with organic solvents as described in Materials and Methods.
[c]ND, not detected.

Gas chromatography/mass spectrometry (GC/MS) of derivatized wood extracts showed that at 4 weeks the colonized wood contained n-hexanal (1,062 ± 220 pmol/g dry weight), *trans*-2-octenal (74 ± 19 pmol/g), and *trans*-2-nonenal (205 ± 42 pmol/g). Non-inoculated wood contained a smaller quantity of n-hexanal (411 ± 199 pmol/g), possibly derived from the peroxidation of aspen wood cell wall lipids, but the other two aldehydes were not detected. The quantities of aldehydes attributable to the fungus were significant relative to fungal membrane lipids, as shown by the ergosterol content of the colonized wood (3,457 ± 338 pmol/g). All values above are means ± sample SD with $n = 3$. Analyses of duplicate cultures at 8 weeks showed that *trans*-2-octenal, *trans*-2-nonenal, and n-hexanal were still present in similar quantities (Table 1). *trans*-2,4-Decadienal was not detected in the colonized wood, but was likely present earlier, since its downstream metabolite n-hexanal was found. *trans*-2-Decenal was not found in any sample. In summary, aspen wood undergoing decay by *G. subvermispora* contained fatty aldehydes which, based on the literature (16, 22–24), probably resulted both from fungal cell membrane peroxidation and from *de novo* production by the fungus. However, it is also possible that the aldehydes resulted from fungal biotransformation of compounds that originated in the wood.

Oxidation of a nonphenolic lignin model dimer

Experiments were done using a ^{14}C-labeled arylglycerol-β-aryl ether-linked lignin model dimer (**I**) with radiochemical detection of the products after separation by high-performance liquid chromatography (HPLC). These reactions, done in acetate buffer without a Mn^{3+}-chelating organic acid, showed that the addition of a *Phanerochaete chrysosporium* MnP isozyme mixture, Mn^{2+}, and *trans*-2,4-decadienal to model **I** resulted in the same co-oxidations that we observed in earlier work using MnP with fatty acids or their esters (Fig. 2) (20). No oxidation occurred in the absence of MnP, Mn^{2+}, or fatty aldehyde. Exogenous H_2O_2 was not required; however, a spectrophotometric assay (32) showed that the *trans*-2,4-decadienal contributed 10 µM peroxides to our reactions.

A time course experiment with *trans*-2-nonenal as the fatty aldehyde showed that it supported the oxidation of model **I** to the same products, and that model **I** removal commenced with no apparent lag (data not shown), in contrast to the lag observed previously using linoleic acid instead as the peroxidizable co-substrate (19). The slower onset in reactions using linoleic acid is consistent with it being located upstream in a sequence that generates reactive aldehydes. However, the difference is probably attributable as well to the fact that our *trans*-2-nonenal preparation contributed a higher concentration of potentially initiating peroxides to the reactions than the linoleic acid did (30 µM vs 5 µM). Attempts to reduce the concentration of endogenous peroxides in

Lignin model	Fatty aldehyde	Products	Quantification method	Reaction time	Product yields
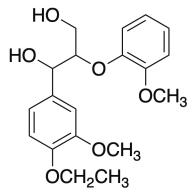 **I** (200 µM)	*trans*-2,4-Decadienal (10 mM)	Uncleaved benzylic ketone (not shown) and polar degradation products including: 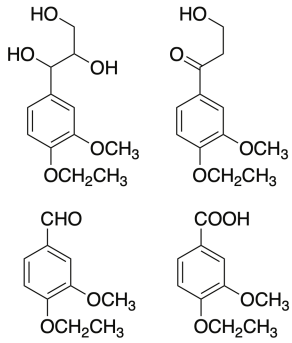	^{14}C-Labeled substrate; HPLC of products with radiochemical detection.	24 h	11% uncleaved ketone 33% polar products
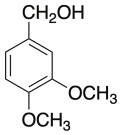 **II** (200 µM)	*trans*-2-Nonenal (10 mM)	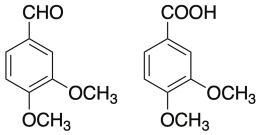	Unlabeled substrate; HPLC of products with diode array determination of UV absorption spectra.	2 h 4 h 24 h	12% aldehyde 1% acid 17% aldehyde 4% acid 19% aldehyde 14% acid

FIG 2 Products formed during the oxidation of lignin model compounds by MnP in the presence of Mn^{2+} and fatty aldehydes.

the *trans*-2-nonenal by reducing them with Fe^{2+} or by preparative HPLC were unsuccessful.

Oxidation of a nonphenolic lignin model monomer

Veratryl alcohol (3,4-dimethoxybenzyl alcohol, **II**) was oxidized in acetate buffer by the *P. chrysosporium* MnP mixture in the presence of fatty aldehydes (Fig. 2). The products were veratraldehyde and veratric acid, as shown by HPLC analysis with diode array UV spectrophotometry. Data are shown here only for *trans*-2-nonenal, but *trans*-2,4-decadienal, *trans*-2-octenal, and n-hexanal gave the same products.

Periodic sampling showed that the ratio of veratric acid to veratraldehyde increased with time (Fig. 2), which suggests that veratraldehyde was also oxidized by the system. As with model **I**, exogenous H_2O_2 was not required, but no reaction occurred in the absence of either MnP, Mn^{2+}, or fatty aldehyde. In complete reaction mixtures, but not those lacking one of the essential ingredients, a brown-black precipitate formed. This result suggests that Mn^{2+} was oxidized to Mn^{3+}, since the latter species disproportionates rapidly in the absence of a stabilizing chelator, yielding Mn^{2+} and insoluble MnO_2 (33).

To determine whether the MnP/fatty aldehyde system might function in the presence of the physiological Mn^{3+} chelator oxalate, we conducted additional oxidations of veratryl alcohol (200 µM initial concentration, 3 h reactions in acetate buffer) in the presence of *trans*-2-nonenal and 1 mM oxalate, which is the approximate concentration of this chelator found earlier in wood colonized for 4–8 weeks by *G. subvermispora* (34). For these experiments, we used recombinant *G. subvermispora* MnP. Oxalate reduced the product yield by about half under these conditions: the summed yield of veratraldehyde and veratric acid was 24 ± 7 µM with 1 mM oxalate vs 43 ± 10 µM without it (95% confidence intervals with $n = 3$; means different by *t* test with $P = 0.003$). No oxidation was detected in control reactions that lacked MnP, Mn^{2+}, or *trans-2*-nonenal.

Exogenous H_2O_2 was not required for the above reactions, and when it was added, the rates did not increase (data not shown). The latter result was expected, because MnP has endogenous catalase activity that becomes significant in slow reactions done with low levels of Mn^{3+} chelators (35). Therefore, we investigated H_2O_2 involvement by testing

the effect of catalase on reactions done in the presence of 1 mM oxalate. In our initial experiment, we found that catalase addition inhibited product formation by more than 95% in a 3-h reaction (data not shown).

To assess the specificity of this effect, we repeated the experiment using both active and heat-inactivated catalase, removed samples at hourly intervals, and assayed them for the two oxidation products by HPLC. Reactions without catalase commenced without a lag, whereas active catalase inhibited the reaction completely for 2 h, after which product formation commenced (presumably due to an instability of the catalase in the reaction mixture). At all times, the results obtained using catalase were significantly lower than the mean values (n = 3) obtained in the control reactions without catalase (t test, $P \leq 0.05$). By contrast, the reaction containing inactivated catalase gave results at all times that were statistically indistinguishable from those obtained in the replicate reactions without catalase (Fig. 3).

No precipitate occurred in reactions that contained 1 mM oxalate, which is consistent with its role as a chelator that stabilizes Mn^{3+}. Inferring that manganic oxalate was formed in these reactions, we tested its ability to oxidize veratryl alcohol in reaction mixtures that contained 400 µM Mn(III) oxalate, 200 µM veratryl alcohol, and 10 mM *trans*-2-nonenal in acetate buffer. Neither veratraldehyde nor veratric acid was detected after 3 h of reaction.

Oxidation of *trans*-2-nonenal

The addition of MnP and Mn^{2+} to *trans*-2-nonenal in acetate buffer resulted in O_2 consumption, as shown by monitoring of sealed reactions using an oxygen electrode (Fig. 4). No reaction occurred when either MnP, Mn^{2+}, or *trans*-2-nonenal was omitted. Exogenous H_2O_2 was not required, but *trans*-2-nonenal contributed 18 µM peroxides to the reaction mixtures. The rate of O_2 uptake in these reactions accelerated until the O_2 in the sealed chamber of the apparatus was nearly exhausted. This result indicates that the reaction generated surplus oxidant beyond that required to maintain a linear rate of MnP turnover.

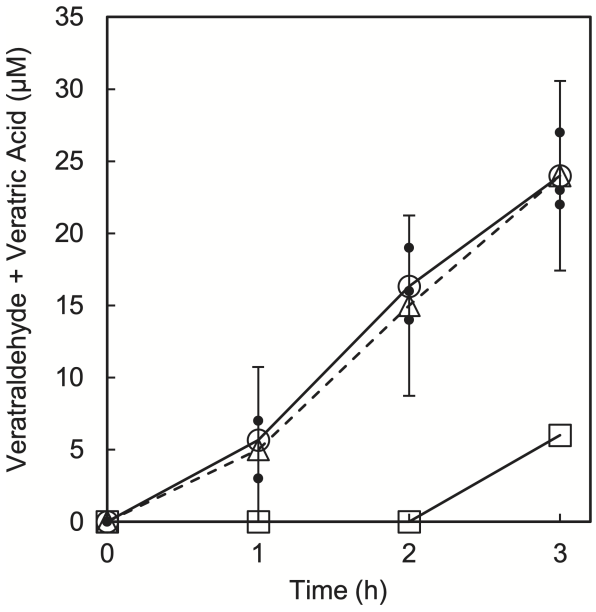

FIG 3 Effect of catalase on the time course of veratryl alcohol oxidation by MnP in the presence of Mn^{2+} and *trans*-2-nonenal. Reactions were conducted in 20 mM Na acetate buffer containing 1 mM Na oxalate (pH 4.5). Circles: without catalase. Error bars show 95% confidence intervals (n = 3). Black points indicate values for the replicates. Squares: with active catalase. Triangles: with heat-inactivated catalase. Extents of oxidation obtained with active catalase are significantly lower than those obtained without catalase with the following values of P: 1 h, 0.051; 2 h, 0.008; and 3 h, 0.007.

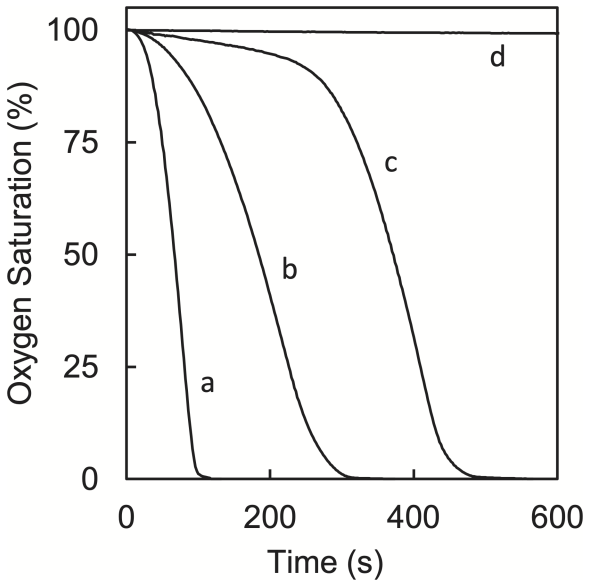

FIG 4 O_2 consumption during reactions of MnP in the presence of Mn^{2+} and *trans*-2-nonenal. Reactions were conducted in 20 mM Na acetate buffer. The traces show reactions using (a) *P. chrysosporium* isozymes and 6.0 mM *trans*-2-nonenal, (b) *P. chrysosporium* isozymes and 4.0 mM *trans*-2-nonenal, (c) *G. subvermispora* MnP 117436 and 6.6 mM *trans*-2-nonenal, and (d) minus MnP with 6.6 mM *trans*-2-nonenal.

The reactions were slower with the recombinant *G. subvermispora* MnP than with the *P. chrysosporium* isozyme mixture, although the total number of enzyme units added was the same in both cases (Fig. 4). O_2 uptake also occurred, but at a slower rate, when the reactions included 1 mM oxalate (data not shown). We did not conduct additional O_2 uptake experiments in the presence of this physiological chelator, because the spontaneous decomposition of manganic oxalate consumes O_2 (36), which would have affected the stoichiometry.

The O_2 uptake results raised the question of what products are formed from *trans*-2-nonenal when it is oxidized by MnP in the presence of Mn^{2+}. The most straightforward route is the one that occurs during transition metal-catalyzed aldehyde autoxidations (25), and would proceed as follows: (i) MnP abstracts the aldehydic hydrogen to give an acyl radical; (ii) O_2 adds to the acyl radical, yielding an acylperoxyl radical. (iii) The acylperoxyl radical abstracts hydrogen from a donor to become *trans*-2-noneneperoxic acid. The likely donor under the conditions of our O_2 uptake experiments is a second molecule of *trans*-2-nonenal. (iv) The peracid then hydrolyzes to give *trans*-2-nonenoic acid and H_2O_2 (37).

We analyzed the *trans*-2-nonenal-derived products of reaction mixtures immediately after O_2 uptake in the sealed reaction chamber was complete. HPLC revealed a single product, which co-eluted with a standard of *trans*-2-nonenoic acid (Fig. 5). A nuclear magnetic resonance (NMR) spectrum of the reaction mixture confirmed this identification: ^{1}H NMR ($CDCl_3$) 5.81 (dt, J = 15.8, 1.5 Hz, 1H, α-H), 7.06 (dt, J = 15.8, 7.2 Hz, 1H, β-H). A comparison of the HPLC results with the O_2 uptake results showed that 1.01 ± 0.06 equivalent (sample SD, n = 3) of *trans*-2-nonenoic acid was produced per equivalent of O_2 consumed.

An alternative pathway for *trans*-2-nonenal oxidation by MnP can be envisaged, in which hydrogen abstraction at C4 instead of C1 would yield a resonance-stabilized radical. However, this route would yield 4-hydroxy-*trans*-2-nonenal or 4-oxo-*trans*-2-nonenal as end products, which were not observed (Fig. 5). Our results appear at variance with those of an earlier study, which reported that some aldehydes supported

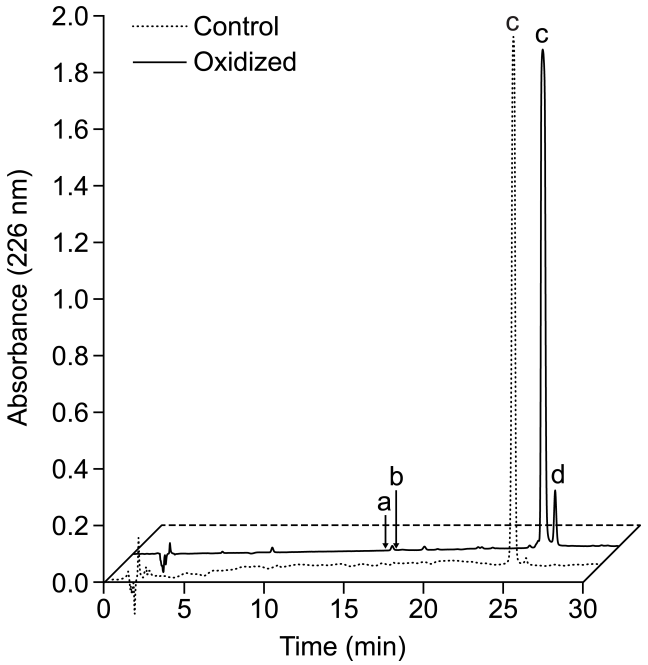

FIG 5 HPLC analysis of reactions done in the presence of *P. chrysosporium* MnPs, Mn^{2+}, and *trans*-2-nonenal. The oxidized sample was analyzed immediately after O_2 consumption in the oxygen electrode cell was complete. The control reaction shown was conducted for the same length of time without MnP. Elution times are indicated for 4-hydroxy-*trans*-2-nonenal (a), 4-oxo-*trans*-2-nonenal (b), *trans*-2-nonenal (c), and *trans*-2-nonenoic acid (d).

the oxidation by MnP of a rubber model compound, yielding a complex mixture of aldehyde-derived degradation products as a result (13).

DISCUSSION

Some variant of the standard MnP catalytic cycle probably has a role in the fatty aldehyde-driven co-oxidations that this enzyme accomplishes, in view of three results we report above: (i) Mn^{2+} was required, (ii) in the absence of oxalate, which stabilizes Mn^{3+}, a precipitate suggestive of insoluble Mn^{4+} was formed, and (iii) catalase was inhibitory. Although exogenous H_2O_2 was not required, our fatty aldehyde preparations already contained low levels of endogenous peroxides. Accordingly, the oxidations we have investigated here may share features with the aldehyde oxidations that are catalyzed by horseradish peroxidase, which initially appeared to be oxidase reactions but are actually peroxidase reactions initiated by peroxide impurities in the aldehydes (38). Nevertheless, it must be said that the diagnostic oxidized states of MnP (Compounds I and II) have not been observed for any of the lipid-dependent biodegradative co-oxidations that it has been reported to accomplish. The necessary experiments would be difficult because the required lipids must be supplied to the reactions as micellar dispersions.

Assuming that the standard catalytic cycle has a role, an additional problem is that the current understanding of MnP turnover mechanisms does not provide a satisfactory explanation for the oxidation of aldehydes. The inhibition rather than stimulation of the reaction by Mn^{3+} chelators, although in line with previous work on MnP-mediated lipid peroxidation (12, 13, 19, 20), appears at variance with the bulk of work on the MnP catalytic cycle. Essentially, there are four possible explanations:

1. Compound I of MnP oxidizes the aldehyde, and Mn^{2+} is then required to reduce the resulting Compound II. This route is unlikely because Compound I oxidizes

either chelated or unchelated Mn^{2+} and then releases the resulting Mn^{3+} with an overall rate constant greater than 10^7 M^{-1} s^{-1}, whereas it oxidizes organic substrates at only about 10^4 M^{-1} s^{-1} (39).
2. Compound I oxidizes Mn^{2+}, and the resulting Compound II then oxidizes the aldehyde instead of oxidizing a second Mn^{2+}. This route is also unlikely because the rate at which Compound II reacts with organic substrates is around 10^2 M^{-1} s^{-1} (39), which would give a turnover of 0.6 s^{-1} under our assay condition of 6 mM *trans*-2-nonenal. By contrast, the rate of Compound II reaction with Mn^{2+} in the presence of oxalate is much higher, saturating at an oxalate concentration near 0.1 mM, such that the rate in physiological (1 mM) oxalate exceeds 200 s^{-1} (40). It is possible that mechanism 2 contributed to fatty aldehyde oxidation in those of our experiments that lacked oxalate, since the rate of Compound II reaction with Mn^{2+} and subsequent release of Mn^{3+} is very low in this case, but it fails to explain the oxidations we observed in 1 mM oxalate. Thus, mechanism 2 lacks physiological relevance.
3. Both Compound I and Compound II oxidize Mn^{2+} exclusively, and the resulting Mn^{3+} oxidizes the aldehyde after release from the enzyme. As we report above, manganic oxalate prepared in acetate buffer did not oxidize veratryl alcohol in the presence of *trans*-2-nonenal. Therefore, this possibility can be excluded.
4. Compound I and Compound II both oxidize Mn^{2+} exclusively, but in the latter case some of the resulting Mn^{3+} oxidizes aldehydes before it can be released from the glutamate and aspartate residues that constitute the MnP binding site for Mn ions (4). Physiological oxalate competes with this process, because it removes some of the Mn^{3+} to give a chelate that is thermodynamically more stable, less electropositive, and consequently less oxidizing. The tendency of Mn^{3+} produced by Compound II of MnP to remain associated with the enzyme in the absence of a chelator such as oxalate is well documented (4, 8, 41). Although it has not been shown that this enzyme-coordinated Mn^{3+} can oxidize substrates, hypothesis 4 is the only one of the four that appears consistent with our data and with the literature. We present it here to encourage further research that may prove or disprove it.

The proposed steps, shown in Fig. 6, incorporate the standard sequence for aldehyde oxidation by transition metal ions (25, 37). The balanced equation for this sequence in conjunction with the MnP catalytic cycle (where R indicates the alkyl sidechain of the aldehyde) is:

$$\mathrm{R{-}CHO + Donor{-}H + O_2 + Mn^{2+} + H^+ \rightarrow R{-}COOH + Donor\bullet + Mn^{3+} + H_2O}$$

The consumption of one O_2 per carboxylic acid produced in this equation agrees with our data. Moreover, the process requires no net input of H_2O_2, also in accordance with our observations. If the electron donor shown is a nonphenolic lignin structure, ligninolysis will ensue, which agrees with our results (Fig. 2).

If the donor is a second molecule of aldehyde instead, it will become a new acyl-peroxyl radical, and the resulting nonenzymatic radical chain reaction of aldehyde oxidations will produce additional H_2O_2 via hydrolysis of the intermediate peracids (Fig. 6). This second route likely explains the rate acceleration we observed in the O_2 uptake experiments, which lacked a lignin model that could have served as an alternate donor. The additional H_2O_2 produced by this mechanism would be expected to increase the oxidation rate, because the concentration of peroxides in our reactions (18 µM), was lower than the K_m of MnP for H_2O_2, which exceeds 100 µM at pH 4.5 (39).

Our results and conclusions are subject to some qualifications. First, the fatty aldehydes we identified are not necessarily the only ones produced by *G. subvermispora* on wood. Extraction of each 10 g colonized wood sample yielded a complex mixture

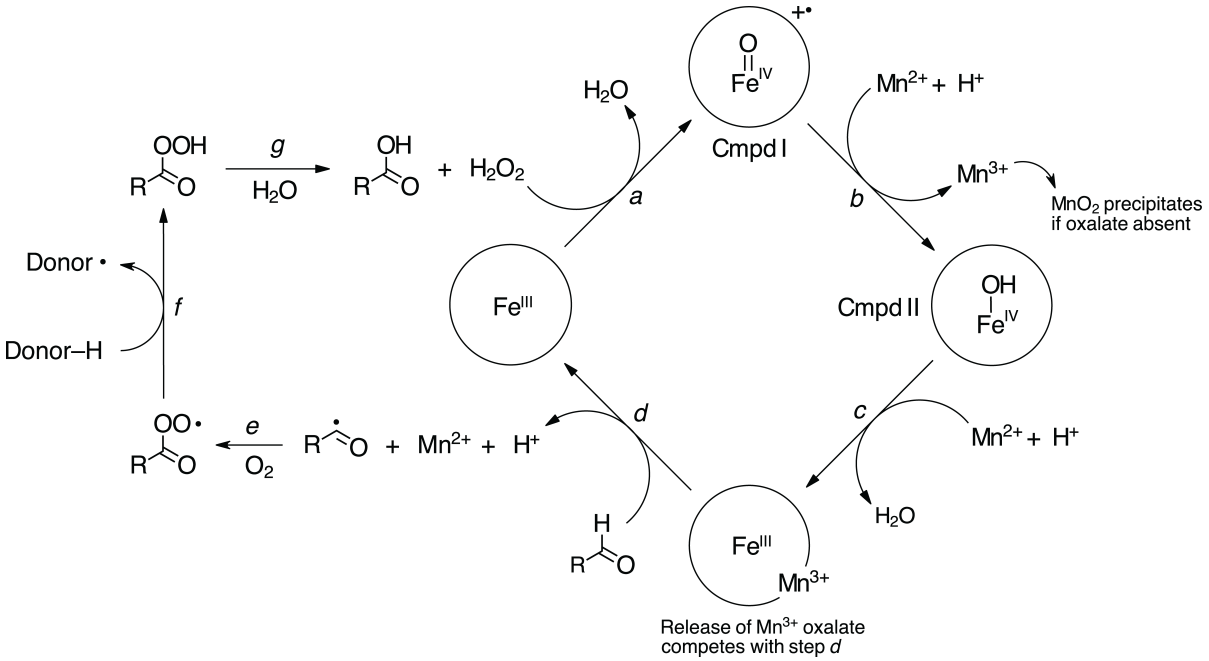

FIG 6 Hypothetical route for generation by MnP of ligninolytic acylperoxyl radicals. Traces of pre-existing H_2O_2 oxidize resting state ferric MnP to Compound I (a), which then oxidizes Mn^{2+} with formation of Compound II (b). The resulting Mn^{3+} is rapidly released, and is stabilized if oxalate is present, but yields an insoluble precipitate in its absence. Compound II then oxidizes a second Mn^{2+}, and some of the resulting Mn^{3+} remains bound to ferric MnP at the physiological oxalate concentration (c). The ferric MnP/Mn^{3+} complex then oxidizes an aldehyde to its acyl radical with release of Mn^{2+} (d). Rapid reaction of the acyl radical with one equivalent of O_2 gives the acylperoxyl radical (e), which subsequently oxidizes a donor molecule to a radical (f) with production of the peracid. If the donor is a lignin structure, production of the radical initiates oxidative biodegradation. The peracid subsequently hydrolyzes to generate the carboxylic acid plus one equivalent of H_2O_2 (g), which replaces the H_2O_2 that was required to initiate the reaction. Abbreviations: Cmpd, Compound. R, Side chain of the aldehyde.

of organic compounds that was not resolved into discrete chromatographic peaks. To identify specific aldehydes by GC/MS, it was necessary to predict which were most likely to occur, and then to look for each by extracting an ion chromatogram at the particular $(M + 1)^+$ mass/charge value for its pentafluorobenzyl oxime derivative. Fatty aldehydes with molecular masses other than those we predicted would have gone undetected.

Second, we cannot say whether the MnP/fatty aldehyde system reproduces the stereoselectivity that *G. subvermispora* exhibits when it degrades arylglycerol-β-aryl ether lignin structures in wood, because our HPLC method did not resolve the diastereomers of model **I**. This fungus removes the *threo* diastereomer more rapidly than it removes the *erythro* diastereomer, which may indicate that the major ligninolytic agent *in vivo* operates via single electron transfer, as opposed to hydrogen atom abstraction (30, 42).

Finally, although our data indicate that acylperoxyl radicals are probably produced from fatty aldehydes by MnP, it is possible that they are not released into solution. If they remain on the enzyme, the production of diffusible acylperoxyl radicals capable of ligninolysis within the wood cell wall would require that the bound radicals initiate a nonenzymatic radical chain reaction in surrounding, dissolved fatty aldehyde molecules. The rate acceleration observed in our O_2 uptake experiments suggests that this reaction can occur (Fig. 4). However, it is not clear that the local concentration of fatty aldehydes in colonized wood is sufficient to sustain it in the vicinity of MnP.

Two previous findings nevertheless suggest that an environment conducive to the production of diffusible lipid-derived peroxyl radicals may exist during white rot. First, MnPs occur on extracellular fungal membranes in colonized wood (43). This juxtaposition may give the enzymes access to water-insoluble fatty acids and fatty aldehydes. Second, *G. subvermispora* produces extracellular glycosphingolipids (44), whose amphipathic structure gives them surfactant activity (45). The lignin-polysaccharide complex in wood likewise exhibits both polar and nonpolar properties (46). Accordingly,

the presence of a biological surfactant might facilitate close contact between MnPs, Mn^{2+}, reactive lipids, and lignin.

MATERIALS AND METHODS

Cultures

Small longitudinal chips of aspen wood (*Populus tremuloides*, approx. 20 × 2 × 2 mm^3) were pre-extracted with acetone to remove low molecular weight extractives and dried in a 55°C oven under vacuum. Portions (10 g dry weight) were autoclaved two times and placed atop potato dextrose agar in Petri dishes (15-cm diameter). The wood in each dish was inoculated with three agar plugs from a culture of *G. subvermispora* 90031-sp (ATCC 90467). The cultures were incubated at 28°C for 4 and 8 weeks. Six replicate cultures were taken at 4 and at 8 weeks for oven-drying and subsequent weight loss assessment. Three cultures were taken at 4 and 8 weeks for assessment of MnP activity. Three cultures at 4 weeks and two cultures at 8 weeks were taken and frozen at −80°C for subsequent extraction of metabolites.

Reagents

Chemicals (from Sigma-Aldrich) were reagent grade with the following exceptions: Fatty aldehydes were analytical standard grade, and organic solvents were pesticide (low residue) grade. Mn(III) oxalate solutions were prepared by dissolving manganese(III) acetate in 100 mM Na oxalate (pH 4.5) in darkness immediately prior to use. Peroxide impurities in fatty aldehydes and in linoleic acid were assayed using a Sigma-Aldrich PeroxiDetect kit (32). The assay detects both H_2O_2 and organic peroxides, and works on the principle that peroxides oxidize Fe^{2+} to Fe^{3+} under acidic conditions. The Fe^{3+} ions then form a colored adduct with xylenol orange, which is quantified by visible spectrophotometry at 560 nm.

A radiolabeled *erythro/threo* mixture of nonphenolic lignin model **I** (1-(4-ethoxy-3-methoxy-*ring*-[^{14}C]phenyl)−2-(2-methoxyphenoxy)−1,3-dihydroxypropane (0.74 mCi $mmol^{-1}$) was prepared and purified by HPLC to greater than 99% chemical and radiochemical purity as described (20). Veratryl alcohol (3,4-dimethoxybenzyl alcohol, model **II**) was vacuum-distilled and dissolved in water at a 10 mM concentration, after which the solutions were flushed with N_2 and frozen for subsequent use (47).

Enzymes

A *P. chrysosporium* MnP isozyme mixture was partially purified from liquid cultures of the fungus by ion exchange column chromatography as described (47). The mixture comprised the isozymes previously named H3, H4, and H5, and exhibited no lignin peroxidase activity.

G. subvermispora MnP was expressed heterologously in *Escherichia coli* BL21(DE3)pLysS. The mature protein-coding sequence of the encoding gene (JGI protein ID# 117436) was manually curated and then synthesized by ATG:biosynthetics (Merzhausen, Germany), after checking whether all the codons had previously been used to express other genes in *E. coli* BL21(DE3)pLysS, and substituting them where required. This sequence was cloned in the expression vector pET23a(+) (Novagen) and the resulting plasmid pET23a-117436 was directly used for expression. *E. coli* DH5α was used for plasmid propagation.

E. coli cells harboring pET-MnP were grown in Terrific Broth containing ampicillin (100 µg/mL) and chloramphenicol (34 µg/mL) with rotary shaking (250 rpm) at 37°C until an OD_{500} of 1.0 was attained. The cultures were induced by the addition of 1.0 mM isopropyl-β-D-thiogalactopyranoside and cultivated for another 4 h at 250 rpm and 37°C. Bacterial pellets harvested by centrifugation were stored at −20°C until processed as described below.

About 15 g of bacterial pellet (wet weight) was suspended in 200 mL of 50 mM Tris–HCl buffer (pH 8.0) containing 10 mM EDTA, 5 mM dithiothreitol (DTT), and 0.1 mg/mL DNase. Cells were disrupted by sonication, and subsequent centrifugation (30 min at 16,000 × *g*) allowed the collection of inclusion bodies containing the MnP polypeptide. Inclusion bodies were washed two times with 20 mM Tris–HCl buffer (pH 8.0) containing 1 mM each of EDTA and DTT. They were then solubilized in the same buffer, containing 8 M urea, at room temperature. Protein concentration was determined by the Bradford method using bovine serum albumin as standard, and then adjusted to 2 mg/mL using the same urea buffer. Subsequent *in vitro* refolding of *G. subvermispora* MnP was performed using 0.16 M urea, 5 mM Ca^{2+}, 20 µM hemin, 0.5 mM oxidized glutathione, 0.1 mM DTT, and 0.1 mg/mL protein, at pH 9.5 overnight (>15 h) in the dark at room temperature (48). Active enzyme was purified by Resource-Q chromatography (GE Healthcare, Chicago, IL), using a 0–300 mM NaCl gradient (20 min, 2 mL min^{-1} flow rate) in 10 mM sodium tartrate (pH 5.5) containing 1 mM $CaCl_2$. The purified MnP was dialyzed against 10 mM sodium tartrate buffer (pH 5.0) and stored at −80°C.

MnP assays of culture extracts

To assess MnP activity in colonized wood, triplicate cultures were each extracted overnight at 4°C with 400 mL of Na tartrate buffer (50 mM, pH 4.5) that contained 100 mM NaCl. Extracts were concentrated by ultrafiltration through a 10-kDa cutoff membrane to *ca*. 5 mL. Na tartrate (50 mM, pH 4.5, 400 mL) was then added and removed by ultrafiltration three times to dialyze the samples. The final concentrates were collected and brought to a volume of 5 mL prior to assaying them. MnP activity was quantified spectrophotometrically as described (41). The reaction mixture (1 mL) contained 50 mM Na tartrate (pH 4.5), 1 mM $MnSO_4$, 0.5 mM 2,6-dimethoxyphenol, and MnP. The reaction was started by adding 0.1 mM H_2O_2. One unit (U) represents 1 µmol of 2,6-dimethoxyphenol dimer (diphenoquinone) formed in 1 min at 25°C.

Metabolite extraction from cultures

All glassware was pre-rinsed before the extractions, using methanol followed by n-hexane. The colonized wood from each culture was placed in a 1-L beaker and stirred overnight in 500 mL methanol. The solvent was decanted and the extraction was repeated with 500 mL chloroform:methanol, 2:1. This solvent was then decanted and another extraction was performed with n-hexane. The methanol and chloroform/methanol extracts were combined, washed with water in a separatory funnel, and dried over granular Na_2SO_4. The hexane extract was separately treated likewise. The organic phases were then combined, filtered, concentrated by rotary vacuum evaporation, transferred to sample vials, and redissolved in several mL of chloroform:methanol, 2:1.

Cyclohexanecarboxaldehyde (1 µg) was added as an internal standard, after which the samples were derivatized to their pentafluorobenzyl oximes using pentafluorobenzyl hydroxylamine as described (49), dried under a stream of N_2, and redissolved in several hundred microliters of CH_2Cl_2. A standard mixture containing an equal weight of each of the predicted aldehydes, cyclohexanecarboxaldehyde, and ergosterol was prepared and derivatized likewise, after which it was redissolved in CH_2Cl_2 to give a concentration of 1 µg mL^{-1} for each compound.

Metabolite analyses

Derivatized metabolites were analyzed by gas chromatography/mass spectrometry using a Varian 3800 gas chromatograph equipped with a 1177 injector, a Varian 4000 ion-trap mass selective detector, and a Combi-Pal autosampler with an SGE 10 µL liquid syringe. A Restek Rxi-5MS column (30-m long, 0.25-mm diameter, and 0.25-µm film thickness) was used with helium as carrier gas at a constant flow of 1 mL min^{-1}. The injection volume for samples and the mixture of standards was 1 µL.

Operating conditions were as follows: The injector temperature was 250°C in split mode (20:1) using a Restek 4 mm, single taper, Siltek injection liner. The oven

temperature program consisted of a 175°C hold for 1 min, a ramp to 225°C at 4 °C min^{-1}, a hold for 1 min, a ramp to 290°C at 20°C min^{-1}, and a hold for 12.25 min. The mass spectrometer was in internal mode, using positive chemical ionization with acetonitrile as the ionization reagent, with a 10 µA emission current, a 250°C transfer line, a 40°C manifold, and a 170°C ion trap operating in full scan mode over the mass/charge (*m/z*) range 175–500.

For metabolite identifications, an extracted ion chromatogram was obtained at the predicted $(M + 1)^+$ value for each compound, and was checked for a match in retention time and peak symmetry to the result obtained for that compound using the mixture of authentic standards. Quantifications were obtained by integrating the peak areas of the extracted ion chromatograms. Mass/charge (*m/z*) values for the $(M + 1)^+$ ions of the derivatized aldehydes were: n-hexanal, 296; *trans*-2-octenal, 322; *trans*-2-nonenal, 336; *trans*-2-decenal, 350; and *trans*-2,4-decadienal, 348. Ergosterol, which was not derivatized, gave a satisfactory chromatography peak with an $(M + 1)^+$ value of 397.

In vitro oxidations of lignin models

Oxidations of lignin model **I** were carried out in loosely capped 6 mL vials on a rotary shaker (120 rpm) at 37°C in the dark. The reactions contained 20 mM Na acetate (pH 4.5), 10 mM emulsified fatty aldehyde, 2% (wt/vol) Tween 20, 0.5 mM $MnSO_4$, 340 µM model **I**, and 0.6 U mL^{-1} of MnP in a total volume of 1–2 mL. Samples were taken, filtered, fractionated by reverse phase HPLC, and analyzed by scintillation counting as described previously (20).

Oxidations of veratryl alcohol were carried out as described above except that 200 µM veratryl alcohol was added in place of model **I**. When oxalate was included, its concentration was 1.0 mM (pH 4.5). When catalase (from *Aspergillus niger*) was included, 1,000 U was added. When heat-inactivated catalase was to be added instead, a 1-mL stock solution of the enzyme was immersed in a boiling water bath for 5 min beforehand. Samples from each veratryl alcohol reaction (250 µL) were taken from the reaction vial at 1 h intervals and subjected to reverse phase HPLC on a Phenomenex Luna C18 (2) column (150-mm long, 4.6-mm diameter, and 5-µm particle size). The column was eluted at 1.0 mL min^{-1} using H_2O/methanol/formic acid, 90:10:0.1 for 5 min, followed by a 25-min linear gradient to H_2O/methanol/formic acid, 40:60:0.1. The eluate was monitored at 280 nm using a Gilson diode array detector, and UV absorption spectra were extracted subsequently for the eluted chromatographic peaks. Veratryl alcohol eluted at 18.1 min, veratraldehyde at 22.3 min, and veratric acid at 22.7 min.

In vitro oxidations of trans-2-nonenal

O_2 uptake during the oxidation of *trans*-2-nonenal was determined with a Yellow Springs Instruments model 5300 oxygen electrode with stirring at 25°C. The electrode was calibrated before each experiment at the same temperature with oxygen-saturated water (260 µM O_2) and Na dithionite-treated water (0 µM O_2). The reactions contained 10 mM Na acetate (pH 4.5), 0.5 mM $MnSO_4$; 6 mM *trans*-2-nonenal; 0.6% (wt/vol) Tween 20; and 0.32 U of MnP in a total volume of 1.6 mL. Reactions were initiated with MnP 3 min after a stable baseline was observed.

To determine the fate of *trans*-2-nonenal after reaction with MnP and Mn(II), samples (50 µL) were withdrawn from the oxygen electrode cell immediately after O_2 uptake was complete, and were subjected to reverse phase HPLC on a Phenomenex Luna C18 (2) column (150-mm long, 4.6-mm diameter, and 5-µm particle size). The column was eluted at 1.0 mL min^{-1} using H_2O/methanol/formic acid, 65:35:0.1, for 1 min, followed by a 37-min linear gradient to methanol/formic acid, 100:0.1. The eluate was monitored at 226 nm. The peak eluting at the position of *trans*-2-nonenoic acid was integrated and quantified relative to chromatograms of a *trans*-2-nonenoic acid standard.

For NMR analysis of the product resulting from MnP-mediated oxidation of *trans*-2-nonenal, reaction mixtures were extracted with $CDCl_3$, dried over granular Na_2SO_4, and analyzed by ^1H NMR spectroscopy using a 500-MHz Bruker Biospin Avance 500

instrument (Billerica, MA) equipped with a cryogenically cooled 5 mm gradient probe with inverse geometry. Spectra were processed using Bruker Topspin 3.1 software.

ACKNOWLEDGMENTS

The authors thank Vitaliy Timokhin for assistance with NMR analysis.

This work was supported by grant DE-SC0006929 from the U.S. Department of Energy, Office of Biological and Environmental Research, to K.E.H. and C.J.H.

AUTHOR AFFILIATIONS

[1]US Forest Products Laboratory, Madison, Wisconsin, USA
[2]Centro de Investigaciones Biológicas "Margarita Salas", Consejo Superior de Investigaciones Científicas, Madrid, Spain
[3]Department of Bacteriology, University of Wisconsin, Madison, Wisconsin, USA

PRESENT ADDRESS

Elena Fernández-Fueyo, Intravacc, De Bilt, Netherlands

AUTHOR ORCIDs

Angel T. Martínez http://orcid.org/0000-0002-1584-2863
Kenneth E. Hammel http://orcid.org/0000-0002-2935-5847

FUNDING

Funder	Grant(s)	Author(s)
U.S. Department of Energy (DOE)	DE-SC0006929	Carl J. Houtman Kenneth E. Hammel

AUTHOR CONTRIBUTIONS

Alexander N. Kapich, Data curation, Investigation, Methodology, Validation, Writing – review and editing | Hideki Suzuki, Data curation, Investigation, Methodology, Validation, Writing – review and editing | Kolby C. Hirth, Data curation, Formal analysis, Investigation, Methodology, Validation, Visualization, Writing – review and editing | Elena Fernández-Fueyo, Data curation, Investigation, Methodology, Validation, Visualization, Writing – review and editing | Angel T. Martínez, Project administration, Resources, Writing – review and editing | Carl J. Houtman, Conceptualization, Data curation, Formal analysis, Funding acquisition, Validation, Writing – review and editing | Kenneth E. Hammel, Conceptualization, Data curation, Formal analysis, Funding acquisition, Investigation, Methodology, Project administration, Resources, Supervision, Validation, Visualization, Writing – original draft, Writing – review and editing

REFERENCES

1. Blanchette RA, Burnes TA, Eerdmans MM, Akhtar M. 1992. Evaluating isolates of *Phanerochaete chrysosporium* and *Ceriporiopsis subvermispora* for use in biological pulping processes. Holzforschung 46:109–116. https://doi.org/10.1515/hfsg.1992.46.2.109
2. Blanchette RA, Krueger EW, Haight JE, Akhtar M, Akin DE. 1997. Cell wall alterations in loblolly pine wood decayed by the white-rot fungus, *Ceriporiopsis subvermispora*. J Biotech 53:203–213. https://doi.org/10.1016/S0168-1656(97)01674-X
3. Boerjan W, Ralph J, Baucher M. 2003. Lignin biosynthesis. Annu Rev Plant Biol 54:519–546. https://doi.org/10.1146/annurev.arplant.54.031902.134938
4. Martínez AT. 2002. Molecular biology and structure-function of ignin-degrading heme peroxidases. Enzyme Microbial Technol 30:425–444. https://doi.org/10.1016/S0141-0229(01)00521-X
5. Lundell TK, Mäkelä MR, Hildén K. 2010. Lignin-modifying enzymes in filamentous basidiomycetes – ecological, functional and phylogenetic review. J Basic Microbiol 50:5–20. https://doi.org/10.1002/jobm.200900338
6. Houtman CJ, Maligaspe E, Hunt CG, Fernández-Fueyo E, Martínez AT, Hammel KE. 2018. Fungal lignin peroxidase does not produce the veratryl alcohol cation radical as a diffusible ligninolytic oxidant. J Biol Chem 293:4702–4712. https://doi.org/10.1074/jbc.RA117.001153
7. Kuan I-C, Tien M. 1993. Stimulation of Mn peroxidase activity: a possible role for oxalate in lignin biodegradation. Proc Natl Acad Sci U S A 90:1242–1246. https://doi.org/10.1073/pnas.90.4.1242
8. Banci L, Bertini I, Dal Pozzo L, Del Conte R, Tien M. 1998. Monitoring the role of oxalate in manganese peroxidase. Biochemistry 37:9009–9015. https://doi.org/10.1021/bi972879+

9. Hofrichter M. 2002. Review: lignin conversion by manganese peroxidase (MnP). Enzyme Microb Tech 30:454–466. https://doi.org/10.1016/S0141-0229(01)00528-2
10. Moen MA, Hammel KE. 1994. Lipid peroxidation by the manganese peroxidase of *Phanerochaete chrysosporium* is the basis for phenanthrene oxidation by the intact fungus. Appl Environ Microbiol 60:1956–1961. https://doi.org/10.1128/aem.60.6.1956-1961.1994
11. Bao W, Fukushima Y, Jensen KA, Moen MA, Hammel KE. 1994. Oxidative degradation of non-phenolic lignin during lipid peroxidation by fungal manganese peroxidase. FEBS Lett 354:297–300. https://doi.org/10.1016/0014-5793(94)01146-x
12. Kapich AN, Steffen KT, Hofrichter M, Hatakka A. 2005. Involvement of lipid peroxidation in the degradation of a non-phenolic lignin model compound by manganese peroxidase of the litter-decomposing fungus *Stropharia coronilla*. Biochem Biophys Res Commun 330:371–377. https://doi.org/10.1016/j.bbrc.2005.02.167
13. Sato S, Ohashi Y, Kojima M, Watanabe T, Honda Y, Watanabe T. 2009. Degradation of sulfide linkages between isoprenes by lipid peroxidation catalyzed by manganese peroxidase. Chemosphere 77:798–804. https://doi.org/10.1016/j.chemosphere.2009.08.014
14. Cunha GGS, Masarin F, Norambuena M, Freer J, Ferraz A. 2010. Linoleic acid peroxidation and lignin degradation by enzymes produced by *Ceriporiopsis subvermispora* grown on wood or in submerged liquid cultures. Enzyme Microb Tech 46:262–267. https://doi.org/10.1016/j.enzmictec.2009.11.006
15. Inoue S, Igarashi Y, Yoneda Y, Kawai S, Okamura H, Nishida T. 2015. Elimination and detoxification of fungicide miconazole and antidepressant sertraline by manganese peroxidase-dependent lipid peroxidation system. Int Biodeterior Biodegrad 100:79–84. https://doi.org/10.1016/j.ibiod.2015.02.017
16. Enoki M, Watanabe T, Nakagame S, Koller K, Messner K, Honda Y, Kuwahara M. 1999. Extracellular lipid peroxidation of selective white-rot fungus, *Ceriporiopsis subvermispora*. FEMS Microbiol Lett 180:205–211. https://doi.org/10.1111/j.1574-6968.1999.tb08797.x
17. Nishimura H, Sasaki M, Seike H, Nakamura M, Watanabe T. 2012. Alkadienyl and alkenyl itaconic acids (ceriporic acids G and H) from the selective white-rot fungus *Ceriporiopsis subvermispora*: a new class of metabolites initiating ligninolytic lipid peroxidation. Org Biomol Chem 10:6432–6442. https://doi.org/10.1039/c2ob25415h
18. Fernandez-Fueyo E, Ruiz-Dueñas FJ, Ferreira P, Floudas D, Hibbett DS, Canessa P, Larrondo LF, James TY, Seelenfreund D, Lobos S, et al. 2012. Comparative genomics of *Ceriporiopsis subvermispora* and *Phanerochaete chrysosporium* provide insight into selective ligninolysis. Proc Natl Acad Sci U S A 109:5458–5463. https://doi.org/10.1073/pnas.1119912109
19. Kapich AN, Korneichik TV, Hatakka A, Hammel KE. 2010. Oxidizability of unsaturated fatty acids and of a non-phenolic lignin structure in the manganese peroxidase-dependent lipid peroxidation system. Enzyme Microb Tech 46:136–140. https://doi.org/10.1016/j.enzmictec.2009.09.014
20. Kapich AN, Jensen KA, Hammel KE. 1999. Peroxyl radicals are potential agents of lignin biodegradation. FEBS Lett 461:115–119. https://doi.org/10.1016/s0014-5793(99)01432-5
21. Spiteller P, Kern W, Reiner J, Spiteller G. 2001. Aldehydic lipid peroxidation products derived from linoleic acid. Biochim Biophys Acta 1531:188–208. https://doi.org/10.1016/s1388-1981(01)00100-7
22. Rapior S, Cavalié S, Andary C, Pélissier Y, Marion C, Bessière J-M. 1996. Investigation of some volatile components of seven fresh wild mushrooms (basidiomycetes). J Essent Oil Res 8:199–201. https://doi.org/10.1080/10412905.1996.9700594
23. Nosaka S, Miyazawa M. 2014. Characterization of volatile components and odor-active compounds in the oil of edible mushroom *Boletopsis leucomelas*. J Oleo Sci 63:577–583. https://doi.org/10.5650/jos.ess13215
24. Fu L, Yang G, Liu L, Ma Y, Zhang X, Zhang X, Li C, Sun Y. 2020. Analysis of volatile components of *Auricularia auricula* from different origins by GC-MS combined with electronic nose. J Food Qual 2020:1–9. https://doi.org/10.1155/2020/8858093
25. Sajus L, de Roch IS. 1980. The liquid phase oxidation of aldehydes, p 89–124. In Bamford CH, Tipper CFH (ed), Comprehensive chemical kinetics. Elsevier.
26. Neta P, Huie RE, Ross AB. 1990. Rate constants for reactions of peroxyl radicals in fluid solutions. J Phys Chem Ref Data 19:413–513. https://doi.org/10.1063/1.555854
27. El-Agamey A, McGarvey DJ. 2002. Acyl/aroylperoxyl radicals: a comparative study of the reactivity of peroxyl radicals resulting from the α-cleavage of ketones. Phys Chem Chem Phys 4:1611–1617. https://doi.org/10.1039/b109309f
28. Watanabe T, Katayama S, Enoki M, Honda Y, Kuwahara M. 2000. Formation of acyl radical in lipid peroxidation of linoleic acid by manganese-dependent peroxidase from *Ceriporiopsis subvermispora* and *Bjerkandera adusta*. Eur J Biochem 267:4222–4231. https://doi.org/10.1046/j.1432-1033.2000.01469.x
29. Akhtar M, Lentz MJ, Blanchette RA, Kirk TK. 1997. Corn steep liquor lowers the amount of inoculum for biopulping. Tappi J 80:161–164.
30. Yelle DJ, Kapich AN, Houtman CJ, Lu F, Timokhin VI, Fort RC, Ralph J, Hammel KE. 2014. A highly diastereoselective oxidant contributes to ligninolysis by the white rot basidiomycete *Ceriporiopsis subvermispora*. Appl Environ Microbiol 80:7536–7544. https://doi.org/10.1128/AEM.02111-14
31. Messner K, Srebotnik E. 1994. Biopulping: an overview of developments in an environmentally safe paper-making technology. FEMS Microbiol Rev 13:351–364. https://doi.org/10.1111/j.1574-6976.1994.tb00054.x
32. Sigma-Aldrich. Peroxidetect kit for the determination of aqueous and lipid hydroperoxides. Technical bulletin. Catalog no. PD1
33. Snider BB, Meunier A, Legault CY. 2012. Manganese(III) acetate. In Encyclopedia of reagents for organic synthesis (EROS). https://doi.org/10.1002/047084289X.rm018.pub2
34. Aguiar A, Souza-Cruz P de, Ferraz A. 2006. Oxalic acid, Fe^{3+}-reduction activity and oxidative enzymes detected in culture extracts recovered from *Pinus taeda* wood chips biotreated by *Ceriporiopsis subvermispora*. Enzyme Microb Tech 38:873–878. https://doi.org/10.1016/j.enzmictec.2004.12.036
35. Timofeevski SL, Aust SD. 1997. Effects of Mn^{2+} and oxalate on the catalatic activity of manganese peroxidase. Biochem Biophys Res Commun 239:645–649. https://doi.org/10.1006/bbrc.1997.7453
36. Jones TJ, Noyes RM. 1983. Mechanistic details of the oxidation of oxalate by manganese(III). J Phys Chem 87:4686–4689. https://doi.org/10.1021/j100246a028
37. Bunton CA, Lewis TA, Llewellyn DR. 1956. Tracer studies in the formation and reactions of organic per-acids. J Chem Soc:1226. https://doi.org/10.1039/jr9560001226
38. Bohne C, MacDonald ID, Dunford HB. 1987. Transient state kinetics of the reactions of isobutyraldehyde with compounds I and II of horseradish peroxidase. J Biol Chem 262:3572–3578. https://doi.org/10.1016/S0021-9258(18)61390-0
39. Whitwam RE, Brown KR, Musick M, Natan MJ, Tien M. 1997. Mutagenesis of the Mn^{2+}-binding site of manganese peroxidase affects oxidation of Mn^{2+} by both compound I and compound II. Biochemistry 36:9766–9773. https://doi.org/10.1021/bi9708794
40. Kishi K, Wariishi H, Marquez L, Dunford HB, Gold MH. 1994. Mechanism of manganese peroxidase compound II reduction effect of organic acid chelators and pH. Biochemistry 33:8694–8701. https://doi.org/10.1021/bi00195a010
41. Wariishi H, Valli K, Gold MH. 1992. Manganese(II) oxidation by manganese peroxidase from the basidiomycete *Phanerochaete chrysosporium*. kinetic mechanism and role of chelators. J Biol Chem 267:23688–23695. https://doi.org/10.1016/S0021-9258(18)35893-9
42. van Erven G, Wang J, Sun P, de Waard P, van der Putten J, Frissen GE, Gosselink RJA, Zinovyev G, Potthast A, van Berkel WJH, Kabel MA. 2019. Structural motifs of wheat straw lignin differ in susceptibility to degradation by the white-rot fungus *Ceriporiopsis subvermispora*. ACS Sustain Chem Eng 7:20032–20042. https://doi.org/10.1021/acssuschemeng.9b05780
43. Daniel G, Goodell B, Jellison J, Paszyzyński A, Crawford R. 1991. Use of monoclonal antibodies to detect Mn(II)-peroxidase in birch wood degraded by *Phanerochaete chrysosporium*. Appl Microbiol Biotechnol 35:674–680. https://doi.org/10.1007/BF00169636
44. Nishimura H, Yamaguchi D, Watanabe T. 2017. Cerebrosides, extracellular glycolipids secreted by the selective lignin-degrading fungus *Ceriporiopsis subvermispora*. Chem Phys Lipids 203:1–11. https://doi.org/10.1016/j.chemphyslip.2016.12.006

45. Dembitsky VM. 2005. Astonishing diversity of natural surfactants: 4. Fatty acid amide glycosides, their analogs and derivatives. Lipids 40:641–660. https://doi.org/10.1007/s11745-005-1427-8
46. Koshijima T, Watanabe T, Yaku F. 1989. Structure and properties of the lignin carbohydrate complex polymer as an amphipathic substance. ACS Symp Ser 397:11–28. https://doi.org/10.1021/bk-1989-0397
47. Tien M, Kirk TK. 1988. Lignin peroxidase of *Phanerochaete chrysosporium*. Methods Enzymol 161:238–249. https://doi.org/10.1016/0076-6879(88)61025-1
48. Fernández-Fueyo E, Ruiz-Dueñas FJ, Miki Y, Martínez MJ, Hammel KE, Martínez AT. 2012. Lignin-degrading peroxidases from genome of selective ligninolytic fungus *Ceriporiopsis subvermispora*. J Biol Chem 287:16903–16916. https://doi.org/10.1074/jbc.M112.356378
49. Kawai Y, Takeda S, Terao J. 2007. Lipidomic analysis for lipid peroxidation-derived aldehydes using gas chromatography-mass spectrometry. Chem Res Toxicol 20:99–107. https://doi.org/10.1021/tx060199e